

Incorporation of horizontal fins into a PCM-based heat sink to enhance the safe operation time: Applicable in electronic device cooling

Sara Rostami^{1,2}, Hossein Mehdizadeh³, Salman Abbasian-Naghneh⁴, Rasool Kalbasi³, Goshtasp Cheraghian^{5, *}, Masoud Afrand^{6,7, *}

1. Laboratory of Magnetism and Magnetic Materials, Advanced Institute of Materials Science, Ton Duc Thang University, Ho Chi Minh City, Vietnam

2. Faculty of Applied Sciences, Ton Duc Thang University, Ho Chi Minh City, Vietnam

3. Department of Mechanical Engineering, Najafabad Branch, Islamic Azad University, Najafabad, Iran

4. Department of Mathematics, Najafabad Branch, Islamic Azad University, Najafabad, Iran

5. Department of Civil Engineering, Technische Universität Braunschweig, Braunschweig, Germany

6. Institute of Research and Development, Duy Tan University, Da Nang 550000, Vietnam

7. Faculty of Electrical – Electronic Engineering, Duy Tan University, Da Nang 550000, Vietnam

* Corresponding author: Masoudafrand@duytan.edu.vn; goshtasp.cheraghian@tu-braunschweig.de

Abstract

In this study, the thermal behavior of a PCM-based heat sink in the presence of horizontal fins was numerically investigated. These types of heat sink can be effective in electronic cooling applications. Independent variables included aspect ratio (AR), number of horizontal fins (n) and their length (LR), while the objective function was defined to maximize the safe operation time (t_{max}). The incorporation of horizontal fins has a positive effect (thermal conductivity enhancement) as well as a negative effect (latent heat reduction). Based on the results, the optimal number of horizontal fins was five. As the number of fins rises up to five, the incremental effect of thermal conductivity improvement (positive effect) was superior to the decremental effect of the latent heat reduction (negative effect), hence the objective function (t_{max}) improved. However, with a further increase in the number of fins upon five, the negative effect prevailed over the positive effect and therefore the safe operation time diminished.

Keywords: PCM-based heat sink. Operation time. Optimal. Horizontal Fin. Aspect ratio

Introduction

Phase change materials (PCMs) have a high ability to store thermal energy [1, 2]. They have high phase change enthalpy, hence during the phase change, absorb a great amount of energy at the low-temperature range (phase change temperature)[3]. It seems that these materials can also be utilized to cool the electronic devices [4] due to their high energy storage capability [5]. Due to the less energy consumption requirements [6, 7], PCMs can be utilized to reduce energy demand in different areas [8]. The conduction heat transfer through PCMs is associated with a high-temperature gradient [9]. The high-temperature gradient makes such materials unable to participate completely in the phase change process. Different techniques have been proposed by researchers to improve the thermal performance of PCMs [10]. Ren et al. [11] performed a numerical study on the potential of microencapsulated phase change material (MEPCM) on holding the temperature increase in electronic devices. They used expanded graphite (EG) nanoparticles with fin to enhance the thermal conductivity of MEPCM, but preliminary results showed that although fin improves the thermal conductivity of the heat sink, it also reduces the latent heat storage capability. They investigated two distinct heat sinks, the first heat sink used fin and the second one utilized EG nanoparticles to improve MEPCM thermal conductivity. In the early stages, the performance of the first heat sink was much better than the second heat sink, but over time, the performance of the second heat sink became better. The authors also showed that if multiple PCM with different melting temperatures were used, thermal performance would be improved. The authors recommend that MEPCM with higher melting temperature t should be used near the heat source. By moving away from the heat source, the MEPCM melting temperature must also be reduced. Emam et al. [12] applied three PCMs of RT25, RT35, and RT44 for cooling of the electronic device under heat fluxes of 2000, 2950 and 3750 W m⁻². They observed that the front temperature for devices which are equipped with PCMs, was lower by 69.8, 80.44, and 74.44°C than the simple device. The authors also investigated the effects of ambient temperature in the solidification duration and it was found that as the ambient temperature increased from 20 to 25°C, the solidification time of RT44HC raised by 94 min. This figure for the ambient temperature of 30°C was 178 min. Farzanehnia et al. [13] used paraffin PCM for the cooling of an electronic chipset. They also added MWCNTs nanoparticles to enhance the PCM thermal conductivity. Three heat sink were prepared and examined to evaluate the effects of using PCM on the electronic device cooling. The first

heat sink was simple, while the second and third ones were equipped with PCM. In the third heat sink, in addition to PCM, nanoparticles of MWCNT were also added. It was found that adding MWCNTs into the paraffin PCM led to a cooling time reduction up to 6%. In the active mode, incorporation of PCM and NPCM reduced the rate of increases in temperature in the early stages of the heating process, while intensified the chipset temperature in the steady state conditions. In the intermittent mode, PCM-based heat sink and NPCM-based heat sink enlarge the operation time while reduced the maximum temperature. Huang et al. [14] conducted many experimental tests to examine the thermal behavior of a novel PCM-based heat sink. They found that some parameters such that PCM thickness, PCM thermal conductivity, heat storage density and finally input power has an impact on the thermal behavior. At high input power, the PCM role in the thermal performance of the heat sink was more obvious than the conditions in which the input power is low. Heat thermal storage improvement led to more operation time of the device prior to reaching the critical temperature. The authors also observed that the PCM thermal conductivity increases the safe operation time slightly. Also, they revealed that the PCM thickness efficacy on the safe operation time was more than the PCM thermal conductivity. Zhao et al. [15] compared the ability of a new low-melting-point alloy (LMPA) with paraffin of RT60 (both of them has approximately the same melting point). LMPA PCM thermal conductivity was 50 times than the RT60 one. Also, LMPA volumetric latent heat storage was 2.1 times that of RT60. Results showed that using LMPA PCM rather than the paraffin enlarged the safe operation time up to 50%. At the same time of operation, the maximum temperature in the heat sink equipped with LMPA was 15°C lower than the RT60 one. Hafiz and Arshad [16] evaluated a PCM-based heat sink equipped with pin fins (fin diameters ranged from 2 to 4mm). A base heat sink (without fin) was also built for comparison. The volume fraction of fins was 9% but the PCM volume fraction was considered variable. In other words, the PCM height varied within the heat sink. According to the results, the 3 mm diameter pin fin have more ability to extend the safe operating time than the other cases. Kalbasi and Salimpour [17] investigated the effect of the number of enclosures on the thermal performance of a PCM-based heat sink (designed for electronics cooling) using constructal design approaches. Independent variables included the number of enclosures, aspect ratio and heat flux while the objective function was defined to enlarge the safe operation time. They showed that thermal performance does not necessarily improve owing to the increase in the number of enclosures (equivalent to complexity in constructal theory). In another study Kalbasi and Salimpour [18], they developed the constructal stages from the first to the second stage by using horizontal fins. They showed that in most cases, four horizontal fins are best suited to maximize the safe operation time. Salimpour et al. [19] applied multi-scale methodology to optimize the number

of enclosures. Using the concept of multi-scale, they put a fin in unheated space in each stage until the objective function (longest safe operation time) reached to the maximum value. Numerical results affirmed that the fin thickness is an effective parameter in finding the optimum number of fins and as the fin thickness decreases, the optimum fin number rises. In other words, for each fin thickness, there is an optimal number of fins.

As mentioned, high-temperature gradients are caused owing to the PCM low conductivity, which eventually reduces the rate of phase change, and it is likely that large amounts of PCM will not melt. Using high conductivity metal fins is a useful approach to improve PCMs thermal conductivity (positive effect). But adding fins rises the system weight as well as the reduction in thermal energy storage potential (negative effect) due to the decrease in volume of materials with high phase change enthalpy (reduced PCM). Therefore, finding the optimal amount of fin is indispensable. The other negative effect of incorporation horizontal fins is the disruption to the convection heat transfer. In this study, the thermal behavior of a PCM-based heat sink in the presence of horizontal fins was numerically investigated. These types of heat sink can be effective in electronic cooling applications. Independent variables included aspect ratio (AR), number of horizontal fins (n) and their length (LR), while the objective function was defined to maximize the safe operation time (t_{max}). Finally, the competition between the positive and negative effects of adding fins will be discussed.

Problem description

As shown in Fig. 1, PCM fills the gap between the horizontal fins. Paraffin wax (Table 1) is considered as PCM. The heat flux enters through the lower surface. Due to the expanding the melted PCM, an empty space above the heat sink is provided.

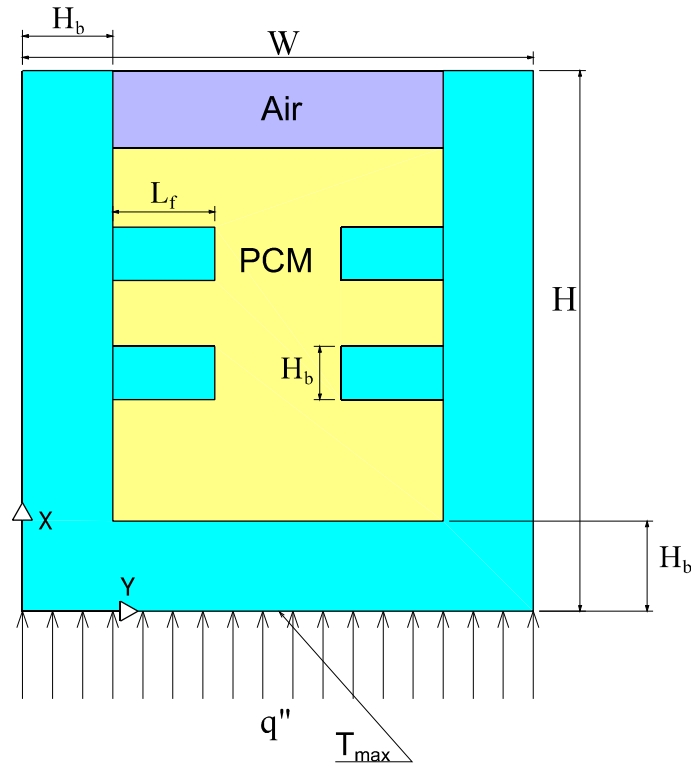


Fig. 1 PCM-based heat sink

Table 1 PCM properties [17]

	$T_l/^{\circ}\text{C}$	$T_s/^{\circ}\text{C}$	$h_{fg}/\text{kJ kg}^{-1}$	$c_p/\text{kJ kg}^{-1} \text{K}^{-1}$		$\mu/\text{kg m}^{-1}\text{s}^{-1}$	$k/\text{W m}^{-1} \text{K}^{-1}$		β/K^{-1}	$\rho/\text{kg m}^{-3}$	
				liquid	solid		liquid	solid		liquid	solid
RT-27	30	28	179	1800	2400	0.00342	0.15	0.24	0.0005	760	870

The density of PCM in the solid state is constant while in the liquid state, it is changed by $\rho = \frac{760}{\beta(T_l - 30) + 1}$. Note that T_l is the liquidus temperature (Table 1). Fins are made of aluminum alloy 6061 with constant thermophysical properties of $c_p = 875 \text{ J kg}^{-1} \text{K}^{-1}$ and $k = 177 \text{ W m}^{-1} \text{K}^{-1}$.

The heat sink height (H) as well as the heat sink area ($A = WH$) is considered to be constant (problem constraint). The applied heat flux changes so that the input energy per the total volume of heat sink remains constant ($\frac{q''_w}{WH} = cte$). The initial temperature is considered to be same as the ambient temperature (27°C). In accordance with Table 1, at 27°C, PCM is in the solid state. All walls (except the lower wall) are considered adiabatic. Because in the worst-case conditions, all energy enter to the heat sink must be absorbed by the cooling system. Note that the boundary condition at the lower surface is $q'' = -k \frac{\partial T}{\partial y}$.

Mathematical formulation

Due to the applications of mathematics in various sciences [20–22], numerical methods were used in this study. Two-phase heat transfer has attracted much research interest [23]. In this study, two-phase heat transfer is also investigated. There are two interfaces in this study [24]. There is an interface between air and PCM, which by applying volume of fluid (VOF) technique, the interface location is estimated. In the VOF technique, the momentum equations along the horizontal and vertical directions with modified properties are used [25]:

$$\begin{aligned} \frac{\partial(\rho u)}{\partial t} + u \frac{\partial(\rho u)}{\partial x} + v \frac{\partial(\rho u)}{\partial y} + w \frac{\partial(\rho u)}{\partial z} \\ = -\frac{\partial P}{\partial x} + \rho g_x + \frac{\partial}{\partial x} \left(\mu \frac{\partial u}{\partial x} \right) + \frac{\partial}{\partial y} \left(\mu \frac{\partial u}{\partial y} \right) + \frac{\partial}{\partial z} \left(\mu \frac{\partial u}{\partial z} \right) + \frac{10^6 (1 - \epsilon)^2}{\epsilon^3 + 0.001} u \end{aligned} \quad (1)$$

$$\begin{aligned} \frac{\partial(\rho v)}{\partial t} + u \frac{\partial(\rho v)}{\partial x} + v \frac{\partial(\rho v)}{\partial y} + w \frac{\partial(\rho v)}{\partial z} \\ = -\frac{\partial P}{\partial y} + \rho g_y + \frac{\partial}{\partial x} \left(\mu \frac{\partial v}{\partial x} \right) + \frac{\partial}{\partial y} \left(\mu \frac{\partial v}{\partial y} \right) + \frac{\partial}{\partial z} \left(\mu \frac{\partial v}{\partial z} \right) + \frac{10^6 (1 - \epsilon)^2}{\epsilon^3 + 0.001} v \end{aligned} \quad (2)$$

Due to the presence of two phases of PCM and air, modified thermophysical properties such as ρ , k and μ can be obtained by the following equations:

$$\rho = \beta_{air} \rho_{air} + (1 - \beta_{air}) \rho_{PCM} \quad (3)$$

$$k = \beta_{air} k_{air} + (1 - \beta_{air}) k_{PCM} \quad (4)$$

$$\mu = \beta_{air} \mu_{air} + (1 - \beta_{air}) \mu_{PCM} \quad (5)$$

In the above equations, β_{air} denote the air volume fraction and obtained by the following Eq:

$$\frac{\partial}{\partial t} [\rho_{Air} \beta_{Air}] + u \frac{\partial}{\partial x} [\rho_{Air} \beta_{Air}] + v \frac{\partial}{\partial y} [\rho_{Air} \beta_{Air}] + w \frac{\partial}{\partial z} [\rho_{Air} \beta_{Air}] = 0 \quad (6)$$

Note that the PCM volume fraction is determined with $\beta_{PCM} = 1 - \beta_{air}$.

The well-known enthalpy-porosity technique is used for the PCM phase change process[26]. In this technique, the interface between solid and liquid is not explicitly tracked. In the enthalpy-porosity approximation, the cell domain is considered as a porous medium and the amount of porosity indicates the liquid fraction (α). The $\alpha = 1$ indicates that the cell temperature is higher than the liquidus temperature ($T \geq T_l$), but the liquid fraction equal to zero indicates that the cell temperature is lower than the solidus temperature ($T \leq T_s$). For the cell temperature is in the range between T_s and T_l , the liquid fraction (α) is between zero and one, and in this case, there is an interface between the liquid and solid phases [27]. The energy equation for problems involving phase change process, the following equations is written as follow:

$$\begin{aligned} \frac{\partial}{\partial t} (\rho h) + \frac{\partial}{\partial x} (\rho u h) + \frac{\partial}{\partial y} (\rho v h) + \frac{\partial}{\partial t} (\rho \Delta H) \\ = \frac{\partial}{\partial x} \left(k \frac{\partial T}{\partial x} \right) + \frac{\partial}{\partial y} \left(k \frac{\partial T}{\partial y} \right) - \frac{\partial}{\partial x} (\rho u \Delta H) - \frac{\partial}{\partial y} (\rho v \Delta H) \end{aligned} \quad (7)$$

where h denote the sensible enthalpy ($h = h_{ref} + \int_{T_{ref}}^T c_p dT$) and ΔH is the latent enthalpy which is related to the amount of liquid fraction $\Delta H = \alpha L$. Note that parameter (L) is the phase change enthalpy.

Second-order upwind and geo reconstruct discretization methods were applied on momentum/energy and liquid fraction equations, respectively. Considering the low velocity in the phase change process, the laminar flow is considered.

Grid study and validation

For grid independency, three networks with interval sizes of 0.2, 0.1 and 0.05 were selected. According to the results, as the interval size decreased from 0.1 to 0.05, results (t_{max}) did not change significantly. Therefore, square meshes at interval size of 0.1 s were chosen. Fig. 2 shows the effect of time step size variation on the output response (t_{max}). As can be seen, there is a sensitivity of the output response to the time stamp, up to $\Delta t = 0.01$ s. As the time step decreases further, the results will not change much.

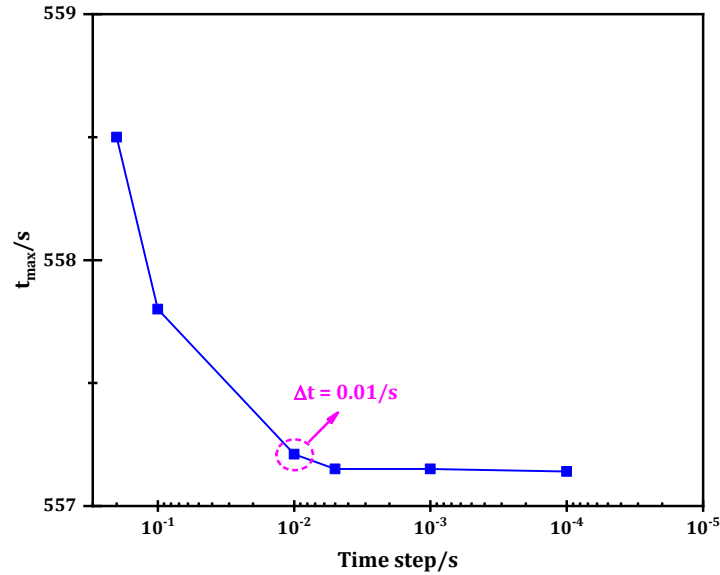


Fig. 2 Independency of the time step size (Δt)

The numerical method used in this study was validated by experiments carried out by Hosseinizadeh et al. [28]. The authors studied a PCM-based heat sink equipped with vertical fins to enhance the heat sink thermal conductivity. The electrical power applied to the bottom wall was 45 W, while the other walls were well insulated. The ambient temperature was 27°C, hence the heat sink initial temperature was 27°C. Applying heat flux on the bottom wall, its temperature begins to rise. The temperature variations of the bottom wall are shown in Fig. 3. As shown, the numerical method can simulate the PCM-based heat sink.

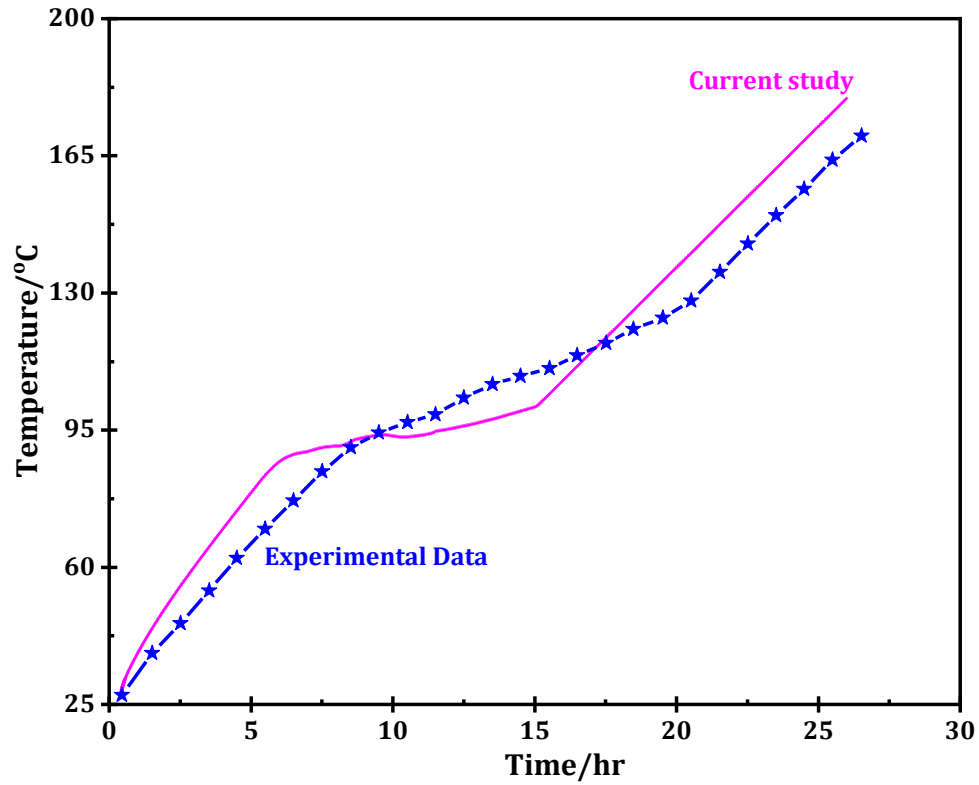


Fig. 3 Comparison between the current study and the experimental data [28]

Results

In general, by loading fins to the PCM, heat transfer within the PCM can be enhanced to maximize the objective function. The objective function is different for various applications. In electronic cooling applications, the objective function is defined as enlarging the safe operation time. For this purpose, given the problem constraints (constant height of the thermal heat sink), the optimal number of horizontal fins within PCM will be examined. The presence of horizontal fins is expected to improve heat distribution within the PCM. For this purpose, two same heat sink with equal dimensions are selected and heat flux is applied to both geometries equally. The variations of t_{max} for a heat sink equipped with horizontal fins and a base heat sink (without horizontal fins) are shown in Fig. 4.

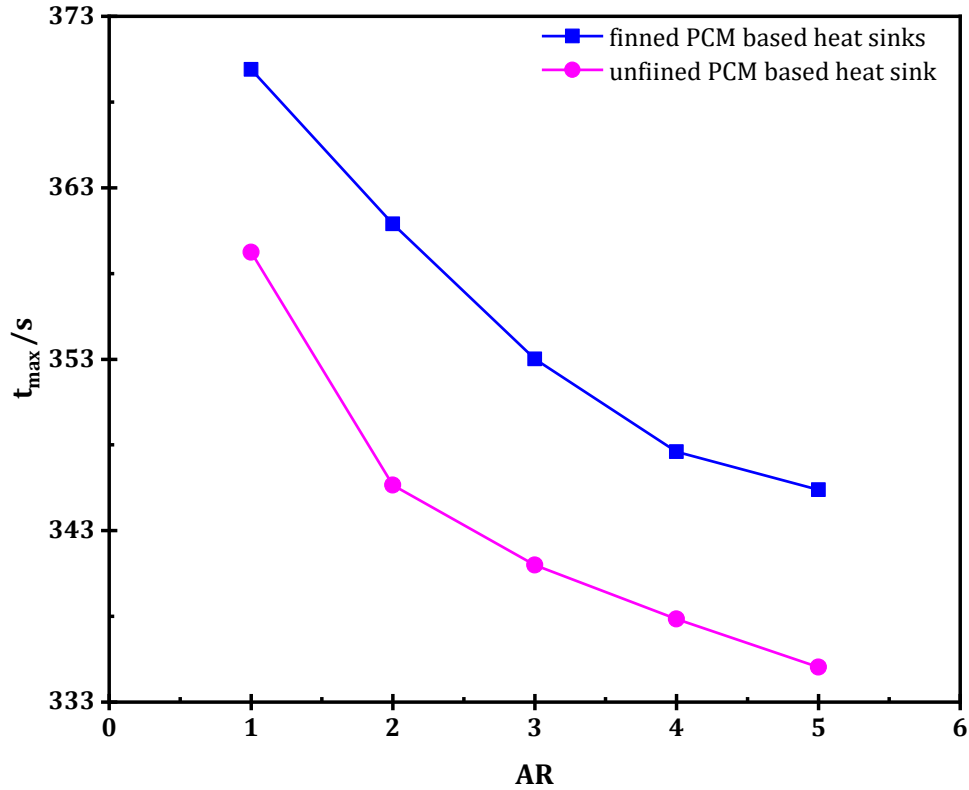


Fig. 4 The variations in t_{max} owing to the incorporation of horizontal fins into the PCM

As can be seen in Fig. 4, by adding horizontal fins, the contact surface between PCM and fins intensified which consequently increased the objective function (t_{max}) in each aspect ratio. The results presented in Fig. 4 are for a heat sink equipped with three fins at length ratio of $LR=0.3$. As can be seen in Fig. 4, as the fins added to the PCM, the contact surface area intensified which consequently improved the heat transfer as well as the increase in t_{max} for each aspect ratio (LR). Therefore, it is desirable to add horizontal fins. To evaluate the effects of the number and length of horizontal fins on heat sink performance, a heat sink at constant height of $H=10\text{ mm}$ is selected. Some horizontal fins at length ratios of $LR = 0.3, 0.5, 0.7$ and 0.9 were loaded at 5000 W m^{-2} applied from the bottom surface. For a heat sink with three horizontal fins ($n=3$), the effects of length ratio on t_{max} are shown in Fig. 5.

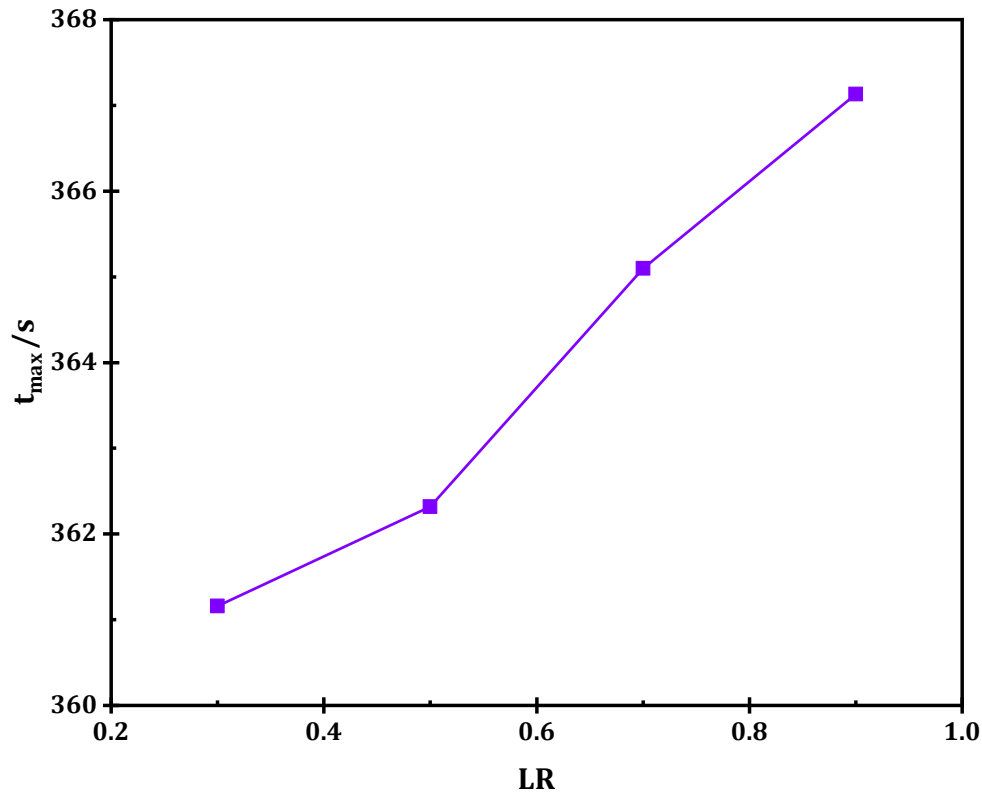


Fig. 5 The effect of increase in length ration (LR) on t_{max} ($H=10\text{ mm}$, $n=3$, $AR=1$)

As shown in Fig. 5, with the rise in the length ratio (equivalent with the fins length growth), t_{max} increases. In Fig. 6, the streamlines are illustrated for both $LR = 0.3$ and $LR = 0.9$. As shown in Fig. 6, as the horizontal fin length rises, the contact area, as well as the convection intensity, increased, hence t_{max} improves.

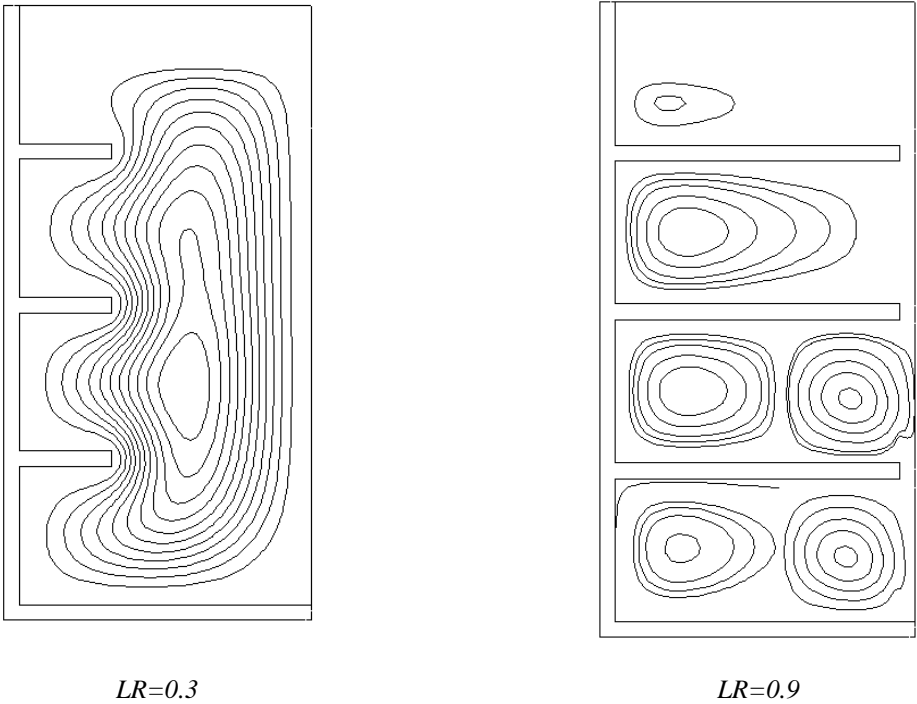


Fig. 6 Comparison of the convection strength between $LR=0.3$ and $LR=0.9$ ($n=3$, $H=10$ mm, $AR=1$)

Now, the number of horizontal fins efficacy is examined. For $n = 5, 11$ and 13 the maximum time is recorded and is shown in Fig. 7.

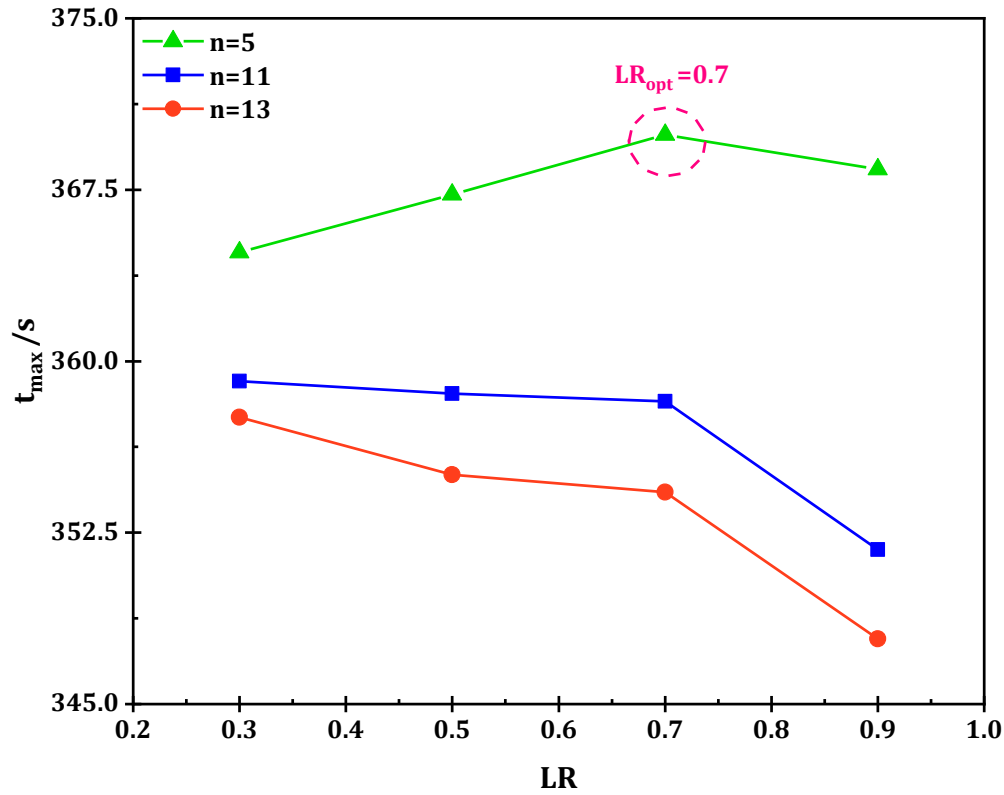


Fig. 7 Effects of length ratio (LR) on t_{max} at different horizontal fins number ($H=10$ mm)

When the number of horizontal fins is five ($n = 5$), increasing the fin length from the $LR=0.3$ to $LR=0.7$ improves the t_{max} , but more increase in LR , diminishes t_{max} . In Fig. 8 the streamlines for the three LR values (0.3, 0.7 and 0.9) are depicted. As can be seen, at length ratio of $LR = 0.7$, the convection is formed in two places (between the horizontal fins and the distance between the horizontal fin tip and the line of symmetry). But at $LR = 0.5$ and $LR = 0.9$ the convection is formed only in one place. Therefore, it seems that the convection strength for $LR=0.7$ is superior to $LR=0.3$ and $LR=0.9$, which consequently the higher objective function.

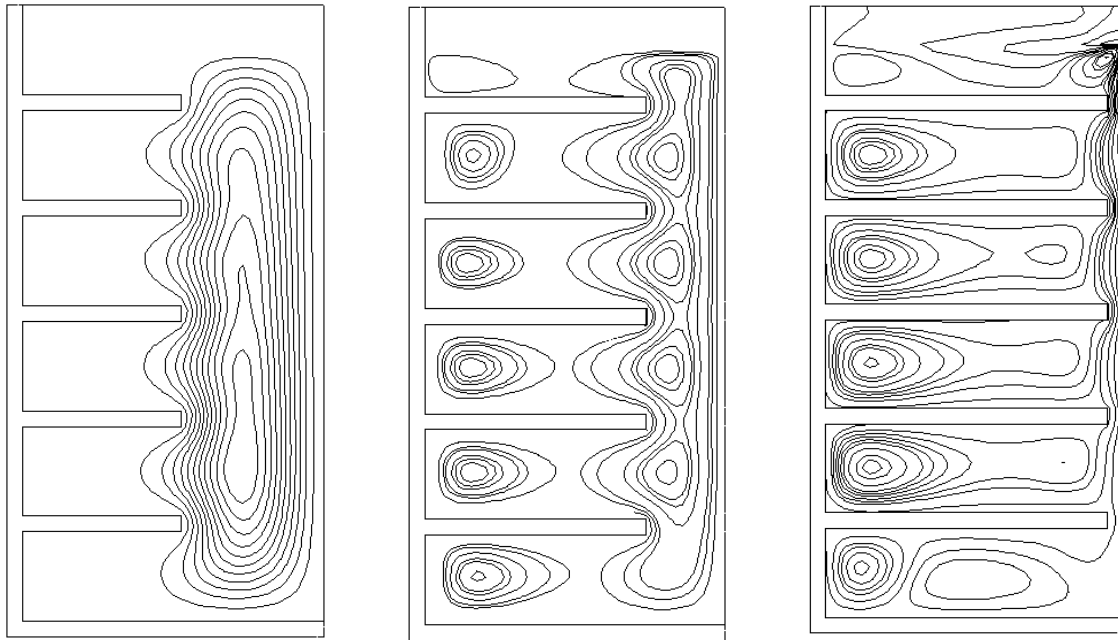
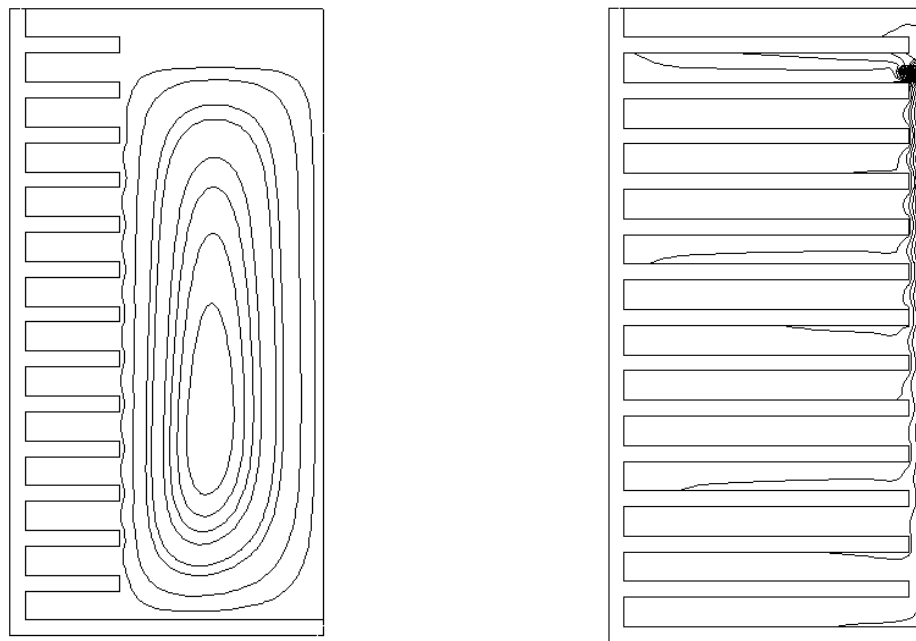


Fig. 8 Convection strength at LR=0.5, 0.7 and 0.9 ($n=5$, $H=10$ mm)

As can be seen in Fig. 9, for heat sink with 13 horizontal fins, increasing the horizontal fin length ratio, reduces the PCM volume. On the other hand, larger fins disrupt the convection. Because as shown in Fig. 9, the rotating cells are diminished owing to increase in fins length, hence the convection intensity reduces. For this reason, t_{max} reduces with increasing fins length with respect to Fig. 7 for heat sink with 13 horizontal fins.

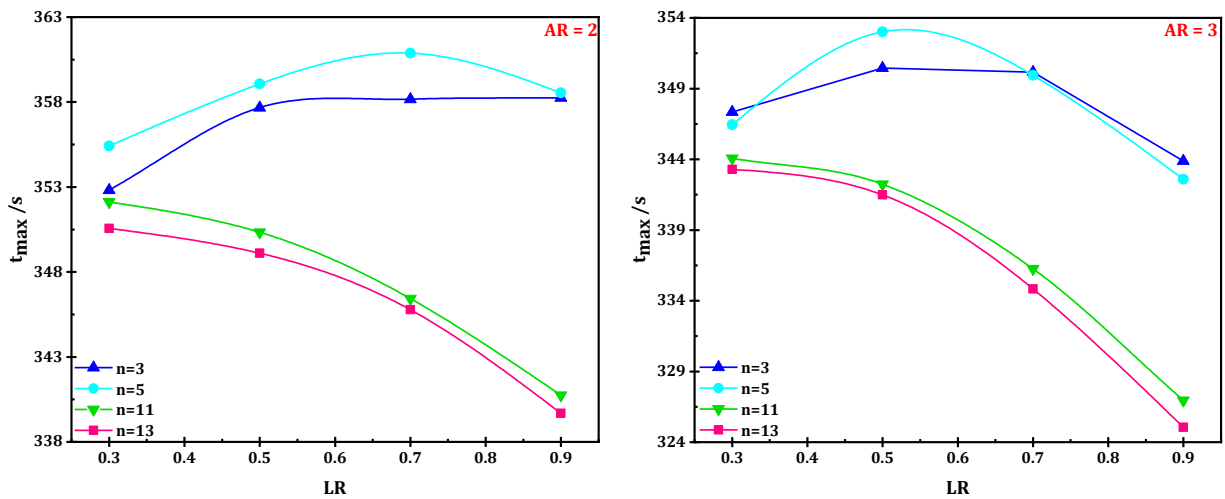


LR=0.3

LR=0.9

Fig. 9 Comparison of strength convection between LR=0.3 and LR=0.9 (n=13, H=10 mm)

Considering the constant heat sink height, as the heat sink width grows, the $AR = \frac{W}{H}$ increases. The effects of increasing AR on t_{max} are shown in Fig. 10. According to Fig. 10, the increase in AR does not affect the number of optimum fins. That is, for $H = 10 \text{ mm}$ from $AR = 1$ to $AR = 5$, the optimal fin number is 5 (i.e., $n_{opt}=5$). As mentioned, adding fin has a positive effect (thermal conductivity enhancement) as well as a negative effect (latent heat reduction). As the number of fins rises up to five, it seems that the incremental effect of thermal conductivity improvement (positive effect) is superior to the decremental effect of the latent heat reduction (negative effect), hence the objective function improved. However, by increasing the number of fins from 5 to 13, the negative effect prevails over the positive effect and therefore the objective function will diminish. As the aspect ratio grows ($AR \uparrow$), the horizontal distance between the vertical walls increases, hence the conduction heat transfer diminished. In this case, convection heat transfer has a larger role in t_{max} . In other words, as AR grows, the role of convection heat transfer in the objective function becomes more important and therefore the optimal length ratio should be reduced. As shown in Fig. 10, the optimal length ratio (LR) decreases with increasing AR .



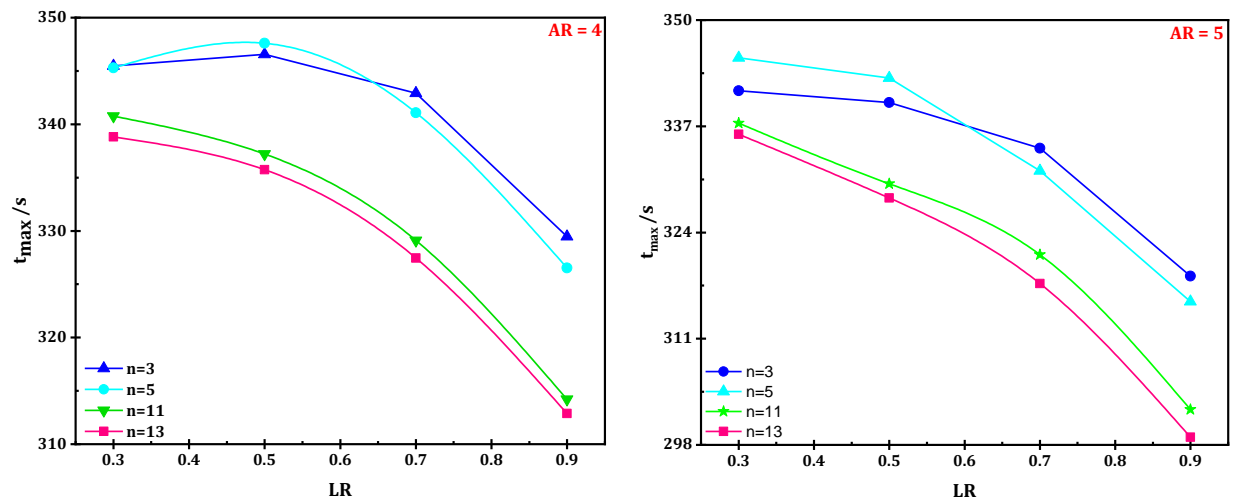


Fig. 10 Optimum fins number at different AR

In accordance with Fig. 10 ($AR=5$), the objective function (t_{max}) diminishes as the length ratio grows. Because at high aspect ratio, convection heat transfer plays a key role, and the shorter the fin length, the greater convection intensity there will be (Fig. 11).

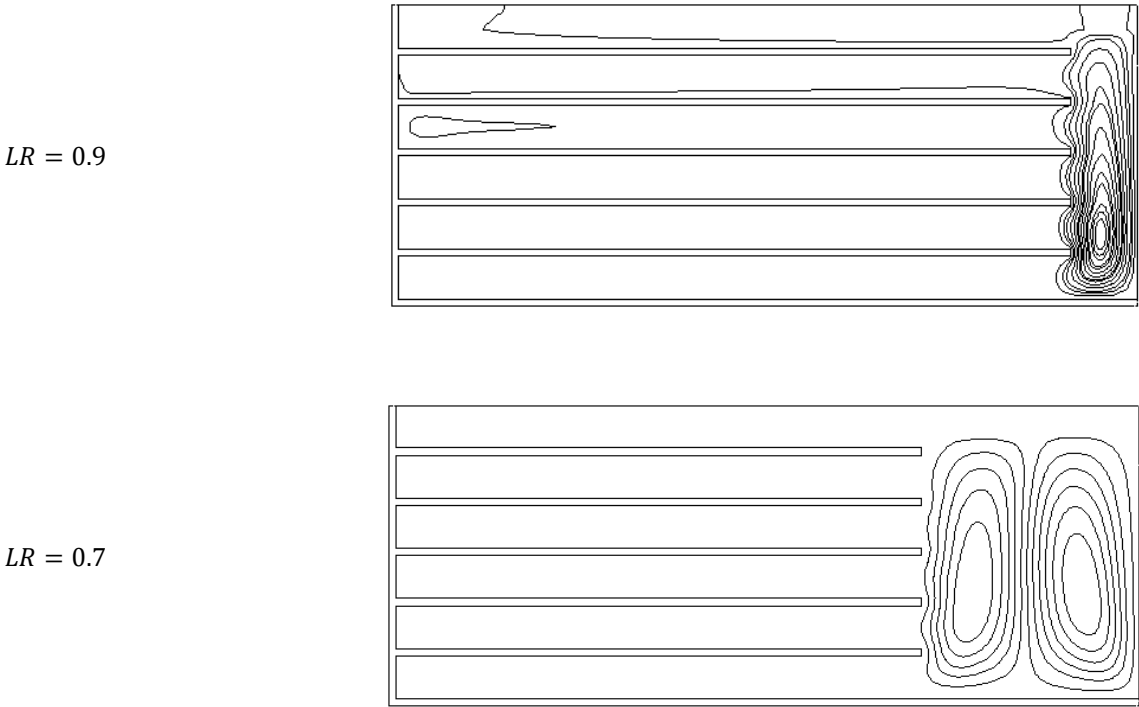


Fig. 11 Streamlines at $LR=0.7$ and $LR=0.9$ ($H=10\text{ mm}$, $n=5$, $AR=5$)

It was mentioned that the optimal fin number for $H = 10\text{mm}$ is five (i.e., $n_{\text{opt}}=5$). Now, the effects of increase in the heat sink height on the number of optimal fins are investigated. The sensitivity of the objective function (t_{max}) to the number of fins (n) and their lengths at different heat sink height of 12.5, 15, 17.5 and 20 mm was illustrated in Fig. 12. According to Fig. 12, the optimal fins number at heights of 12.5, 15, 17.5 and 20 mm is also five (i.e., $n_{\text{opt}} = 5$). It seems that by increasing the number of fins up to five, the positive effect of fin installation was superior to its negative effect, but by increasing the number of fins from 5 to 13, the negative effect (decreasing the phase change enthalpy) overcomes the positive effect (increase in thermal conductivity), hence decreases t_{max} . Increasing the height parameter at $AR = 1$ has no effect on the optimum length (L_{opt}) and focusing on Fig. 12 revealed that (L_{opt}) is 0.7.

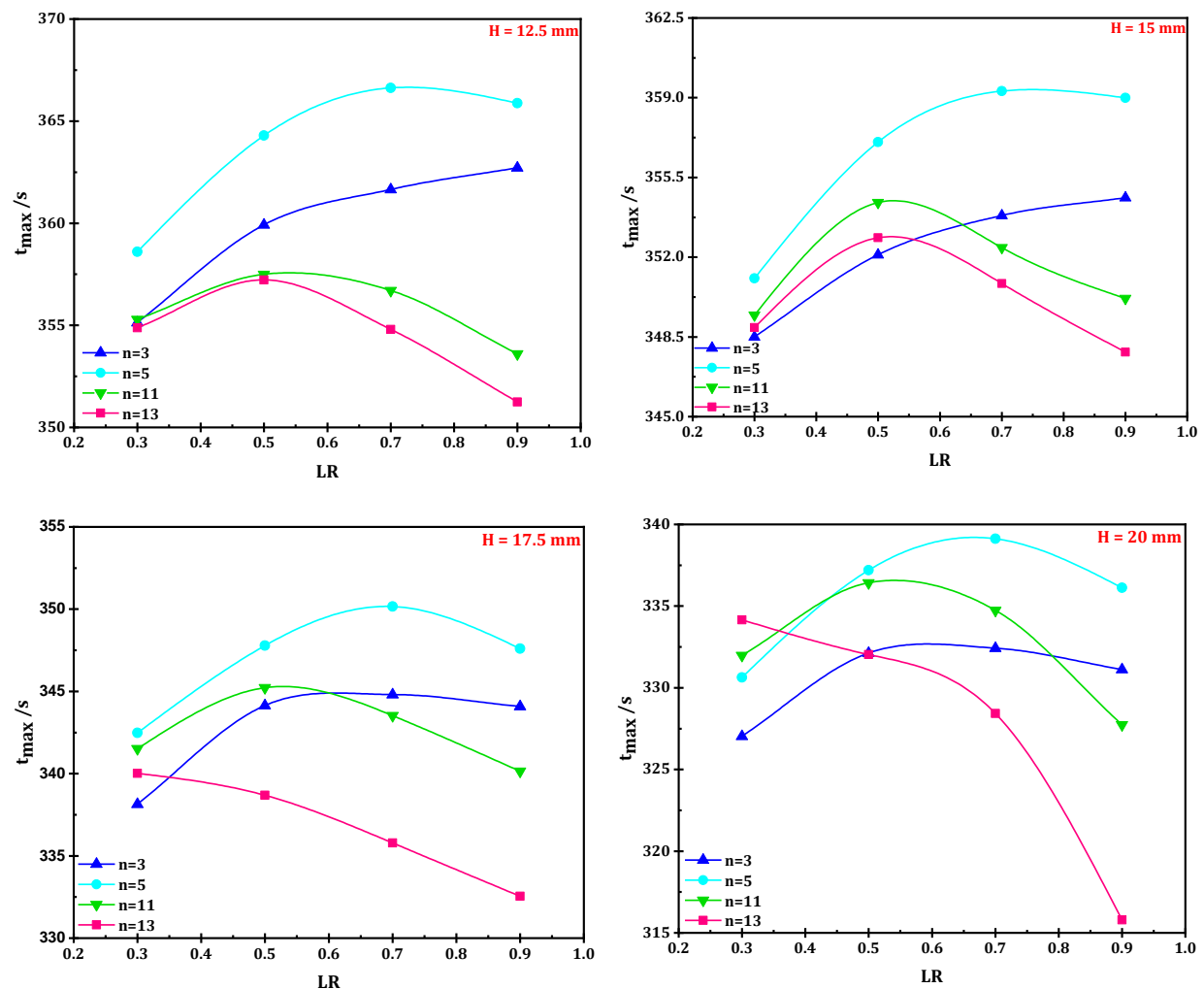


Fig. 12 The variation in t_{max} with respect to LR at different heat sink height

Conclusions

In this study, the thermal behavior of a PCM-based heat sink in the presence of horizontal fins was numerically investigated. These types of heat sink can be effective and useful in electronic cooling applications. Since the heat sink width was considered variable, the heat flux is varied so that the heat sink energy input was the same for each heat sink. The most important results are as follows:

- Adding horizontal fins, the contact surface and consequently heat distribution through the heat sink improved. But at the same time, it reduced the movement of the liquid phase and hence disrupted the convection. Hence, t_{\max} depends on the horizontal fins number. The results showed that for each heat sink there is an optimal number of horizontal fins, which further increases in the number of fins diminished t_{\max} .
- Based on the results, for $AR=1$ to $AR=5$, the optimal number of horizontal fins was five. As the number of fins rises up to five, the incremental effect of thermal conductivity improvement (positive effect) was superior to the decremental effect of the latent heat reduction (negative effect), hence the objective function improved. However, for number of fins from 5 to 13, the negative effect prevailed over the positive effect and therefore the safe operation time diminished.
- As the aspect ratio grows ($AR \uparrow$), the horizontal distance between the vertical walls increases, hence the conduction heat transfer diminishes. In this case, convection heat transfer has a larger role in safe operation time. As the aspect ratio increased from 1 to 5, the optimal length ratio decreased from 0.7 to 0.3. With the growth in AR , the role of convection heat transfer in the objective function becomes more important, hence the optimal length ratio should have a lower value.
- Heat sink width has a greater effect on the optimal fins number as well as the optimal fins length than the heat sink height.

References

- [1] L. Klimeš *et al.*, "Computer modelling and experimental investigation of phase change hysteresis of PCMs: The state-of-the-art review," *ApEn*, vol. 263, p. 114572, 2020/04/01/ 2020, doi: <https://doi.org/10.1016/j.apenergy.2020.114572>.
- [2] J. Jeon, J.-H. Lee, J. Seo, S.-G. Jeong, and S. Kim, "Erratum to: Application of PCM thermal energy storage system to reduce building energy consumption," *Journal of Thermal Analysis and Calorimetry*, vol. 116, no. 1, pp. 539-539, 2014/04/01 2014, doi: 10.1007/s10973-012-2408-1.
- [3] N. Beemkumar, D. Yuvarajan, M. Arulprakasajothi, K. Elangovan, and T. Arunkumar, "Control of room temperature fluctuations in the building by incorporating PCM in the roof," *Journal of Thermal Analysis and Calorimetry*, 2020/01/03 2020, doi: 10.1007/s10973-019-09226-0.
- [4] S. Rashidi, H. Shamsabadi, J. A. Esfahani, and S. Harmand, "A review on potentials of coupling PCM storage modules to heat pipes and heat pumps," *Journal of Thermal Analysis and Calorimetry*, vol. 140, no. 4, pp. 1655-1713, 2020/05/01 2020, doi: 10.1007/s10973-019-08930-1.
- [5] S. K. Sahoo, M. K. Das, and P. Rath, "Application of TCE-PCM based heat sinks for cooling of electronic components: A review," *Renewable and Sustainable Energy Reviews*, vol. 59, pp. 550-582, 2016/06/01/ 2016, doi: <https://doi.org/10.1016/j.rser.2015.12.238>.
- [6] M. Yari, R. Kalbasi, and P. Talebizadehsardari, "Energetic-exergetic analysis of an air handling unit to reduce energy consumption by a novel creative idea," *International Journal of Numerical Methods for Heat & Fluid Flow*, vol. 29, pp. 3959-3975, 2019.
- [7] R. Kalbasi, A. Shahsavari, and M. Afrand, "Reducing AHU energy consumption by a new layout of using heat recovery units," *Journal of Thermal Analysis and Calorimetry*, vol. 139, no. 4, pp. 2811-2820, 2020/02/01 2020, doi: 10.1007/s10973-019-09070-2.
- [8] Y. Yang, W. Wu, S. Fu, and H. Zhang, "Study of a novel ceramsite-based shape-stabilized composite phase change material (PCM) for energy conservation in buildings," *Construction and Building Materials*, vol. 246, p. 118479, 2020/06/20/ 2020, doi: <https://doi.org/10.1016/j.conbuildmat.2020.118479>.
- [9] X. Huang, C. Zhu, Y. Lin, and G. Fang, "Thermal properties and applications of microencapsulated PCM for thermal energy storage: A review," *Appl. Therm. Eng.*, vol. 147, pp. 841-855, 2019/01/25/ 2019, doi: <https://doi.org/10.1016/j.applthermaleng.2018.11.007>.
- [10] L.-L. Tian, X. Liu, S. Chen, and Z.-G. Shen, "Effect of fin material on PCM melting in a rectangular enclosure," *Appl. Therm. Eng.*, vol. 167, p. 114764, 2020/02/25/ 2020, doi: <https://doi.org/10.1016/j.applthermaleng.2019.114764>.
- [11] Q. Ren, P. Guo, and J. Zhu, "Thermal management of electronic devices using pin-fin based cascade microencapsulated PCM/expanded graphite composite," *International Journal of Heat and Mass Transfer*, vol. 149, p. 119199, 2020/03/01/ 2020, doi: <https://doi.org/10.1016/j.ijheatmasstransfer.2019.119199>.
- [12] M. Emam, S. Ookawara, and M. Ahmed, "Thermal management of electronic devices and concentrator photovoltaic systems using phase change material heat sinks: Experimental investigations," *Renewable Energy*, vol. 141, pp. 322-339, 2019/10/01/ 2019, doi: <https://doi.org/10.1016/j.renene.2019.03.151>.
- [13] A. Farzanehnia, M. Khatibi, M. Sardarabadi, and M. Passandideh-Fard, "Experimental investigation of multiwall carbon nanotube/paraffin based heat sink for electronic device thermal management," *Energy Convers. Manage.*, vol. 179, pp. 314-325, 2019/01/01/ 2019, doi: <https://doi.org/10.1016/j.enconman.2018.10.037>.
- [14] Z. Huang *et al.*, "Experimental and numerical study on thermal performance of Wood's alloy/expanded graphite composite phase change material for temperature control of electronic

- devices," *International Journal of Thermal Sciences*, vol. 135, pp. 375-385, 2019/01/01/ 2019, doi: <https://doi.org/10.1016/j.ijthermalsci.2018.09.031>.
- [15] L. Zhao, Y. Xing, Z. Wang, and X. Liu, "The passive thermal management system for electronic device using low-melting-point alloy as phase change material," *Appl. Therm. Eng.*, vol. 125, pp. 317-327, 2017/10/01/ 2017, doi: <https://doi.org/10.1016/j.applthermaleng.2017.07.004>.
- [16] H. M. Ali and A. Arshad, "Experimental investigation of n-eicosane based circular pin-fin heat sinks for passive cooling of electronic devices," *International Journal of Heat and Mass Transfer*, vol. 112, pp. 649-661, 2017/09/01/ 2017, doi: <https://doi.org/10.1016/j.ijheatmasstransfer.2017.05.004>.
- [17] R. Kalbasi and M. R. Salimpour, "Constructal design of phase change material enclosures used for cooling electronic devices," *Applied Thermal Engineering*, vol. 84, pp. 339-349, 2015/06/05/ 2015, doi: <https://doi.org/10.1016/j.applthermaleng.2015.03.031>.
- [18] R. Kalbasi and M. R. Salimpour, "Constructal design of horizontal fins to improve the performance of phase change material rectangular enclosures," *Applied Thermal Engineering*, vol. 91, pp. 234-244, 2015/12/05/ 2015, doi: <https://doi.org/10.1016/j.applthermaleng.2015.08.024>.
- [19] M. R. Salimpour, R. Kalbasi, and G. Lorenzini, "Constructal multi-scale structure of PCM-based heat sinks," *Continuum Mechanics and Thermodynamics*, vol. 29, no. 2, pp. 477-491, 2017/03/01 2017, doi: 10.1007/s00161-016-0541-y.
- [20] M. Rafiee and S. Abbasian-Naghneh, "E-learning: Development of a model to assess the acceptance and readiness of technology among language learners," *Computer Assisted Language Learning*, pp. 1-21, 2019.
- [21] S. Abbasian-Naghneh, "Global malmquist productivity index based on preference common-weights," *Filomat*, vol. 30, no. 10, pp. 2653-2661, 2016.
- [22] M. Rafiee and S. Abbasian-Naghneh, "Prioritization of critical individual factors influencing willingness to communicate: AHP method," *Journal of Multilingual and Multicultural Development*, vol. 40, no. 6, pp. 461-474, 2019.
- [23] R. Kalbasi, F. Izadi, and P. Talebizadehsardari, "Improving performance of AHU using exhaust air potential by applying exergy analysis," *Journal of Thermal Analysis and Calorimetry*, vol. 139, no. 4, pp. 2913-2923, 2020/02/01 2020, doi: 10.1007/s10973-019-09198-1.
- [24] B. Ding, Z.-H. Qi, C.-S. Mao, L. Gong, and X.-L. Liu, "Numerical investigation on cooling performance of PCM/cooling plate hybrid system for power battery with variable discharging conditions," *Journal of Thermal Analysis and Calorimetry*, 2020/04/01 2020, doi: 10.1007/s10973-020-09611-0.
- [25] V. R. Voller, M. Cross, and N. Markatos, "An enthalpy method for convection/diffusion phase change," *International journal for numerical methods in engineering*, vol. 24, no. 1, pp. 271-284, 1987.
- [26] T. Bouzennada, F. Mechighel, A. Filali, and L. Kolsi, "Study of the usability of sinusoidal function heat flux based on enthalpy-porosity technique for PCM-related applications," *Journal of Thermal Analysis and Calorimetry*, 2020/01/03 2020, doi: 10.1007/s10973-019-09192-7.
- [27] C. Swaminathan and V. R. Voller, "A general enthalpy method for modeling solidification processes," *Metallurgical transactions B*, vol. 23, no. 5, pp. 651-664, 1992.
- [28] S. F. Hosseinzadeh, F. L. Tan, and S. M. Moosania, "Experimental and numerical studies on performance of PCM-based heat sink with different configurations of internal fins," *Appl. Therm. Eng.*, vol. 31, no. 17, pp. 3827-3838, 2011/12/01/ 2011, doi: <https://doi.org/10.1016/j.applthermaleng.2011.07.031>.